HYDROLOGICAL PROCESSES
Hydrol. Process. **15**, 183–199 (2001)

Investigating mechanisms of stormflow generation by natural tracers and hydrometric data: a small catchment study in the Black Forest, Germany

E. Hangen,[1]* M. Lindenlaub,[1] Ch. Leibundgut[1] and K. von Wilpert[2]

[1] *Institute of Hydrology, Albert-Ludwigs-University Freiburg, Fahnenbergplatz, 79085 Freiburg, Germany*
[2] *Department of Soil Science and Forest Nutrition, Forest Research Institute Baden-Württemberg, Wonnhaldestr. 4, 79100 Freiburg, Germany*

Abstract:

The importance and interaction of various hydrological pathways and identification of runoff source areas involved in solute transport are still under considerable debate in catchment hydrology. To reveal stormflow generating areas and flow paths, hydrometric behaviour of throughfall, soil water from various depths, runoff, and respective concentrations of the environmental tracers ^{18}O, Si, K, SO_4 and dissolved organic carbon were monitored for a 14-week period in a steep headwater catchment in the Black Forest Mountains, Germany.

Two stormflow hydrographs were selected and, based on ^{18}O and Si, chemically separated into three flow components. Their sources were defined using mixing diagrams. Additional information about stormflow generating mechanisms was derived from recession analyses of the basin's complete 5-year hydrograph record. By providing insight into storage properties and residence times of outflowing reservoirs of the basin, recession analysis proved to be a valuable tool in runoff model conceptualization. Its results agreed well with hydrometric and hydrochemical data. Supported by evaluation of 30 hillslope soil profiles a coherent concept of stormflow generation could be derived: whereas in many steeply sloped basins in the temperate region soil water from hillslopes appears to have an immediate effect on the shape of the stormflow hydrograph, its role at this basin is basically restricted to the recharge of the groundwater reservoir in the near-channel area. Storm hydrograph peaks appear to be derived from a small direct runoff component supplemented by a fast delivery of baseflow from the groundwater reservoir in the valley bottom.
Copyright © 2001 John Wiley & Sons, Ltd.

KEY WORDS tracers; conceptual runoff model; recession analysis; hydrograph separation; mixing analysis

INTRODUCTION

During the last few decades new methods in tracer hydrology have improved substantially our understanding of runoff producing processes (Kendall and McDonnell, 1998). In particular the use of stable isotopes as tracers used in combination with hydrograph separation techniques was an important component in this development (e.g. Peters *et al*., 1995). For many areas in humid, temperate climates the dominance of pre-event water in storm runoff production is well documented (Rice and Hornberger, 1998), as is the role of soil water in storm and snowmelt runoff (e.g. McGlynn *et al*., 1999). The origin and contribution of surface, near-surface and macropore flow to single runoff events is verified for selected areas. For these, models of basin response also can be conceptualized that are consistent with the chemical and physical characteristics of drainage basins, and which describe specific runoff mechanisms such as 'saturated pipe flow' (McDonnell, 1990), 'rapid surface water mixing' (Waddington *et al*., 1993), or 'continuous open system isotope mixing' (Harris *et al*., 1995).

* Correspondence to: E. Hangen, Department of Soil Protection and Recultivation, Brandenburg University of Technology, Cottbus, PO Box 101344, 03013 Cottbus, Germany. E-mail: hangen@tu-cottbus.de

Received 11 December 1997
Accepted 28 February 2000

Copyright © 2001 John Wiley & Sons, Ltd.

In addition to these findings several authors (Sklash *et al*., 1986; Wilson *et al*., 1990; Rice and Hornberger, 1998) have stated the need for integrated tracer studies, which utilize analytical procedures of hydrograph evaluation based on hydrometric and additional basin-related data. The significance of soil water in stormflow generation, as suggested by hydrochemical data, was confirmed by extensive hydrometric data for a temperate forested headwater catchment (Bazemore *et al*., 1994). In an Arctic watershed a two-component runoff system derived from chemical separations of storm hydrographs well agreed with graphical separation techniques applied at recession curves (McNamara *et al*., 1997). Based on such experimental results, runoff generating processes were described in simulation models, for instance, groundwater ridging by HECNAR (Jayatilaka and Gillham, 1996) and runoff processes on the basin-scale by topographically based simulations such as TOPMODEL (e.g. Güntner *et al*., 1999) and others.

Runoff generation mechanisms are difficult to generalize from one basin to another and even from storm to storm within the same basin (Jenkins *et al*., 1994). For instance, intrabasin stream chemistry can be associated with different degrees of reforestation (Havel *et al*., 1999), and solute concentration of subsurface flow can vary depending on the spatially variable flushing frequency (Burns *et al*., 1998), which both may affect the interpretation of chemical hydrograph separations in forested basins.

The single-event analysis based upon tracer data is often constrained by fundamental limitations in the temporal and spatial context of the data (Hinton *et al*., 1994). Regarding this, McDonnell (1990) and others have emphasized the importance of antecedent soil moisture in determining runoff generating processes.

The objective of this study is to identify stormflow generating processes in a headwater catchment and to conceptualize a stormflow runoff model based on a variety of experimental data. In contrast to most previous integrated tracer investigations, which mainly limit their reflections on chemical hydrograph separations combined with hydrometric data, this study additionally incorporates data of recession analyses as well as chemographs of characteristic natural tracers. The aim of applying recession analyses is to consider the basin's storage properties and outflowing reservoirs in order to further justify the chosen number of runoff components used in stormflow hydrograph separations and to gain insight into the temporal process of stormflow generation.

STUDY AREA

The study was conducted in the 9·3 ha Conventwald basin (Figure 1) in the Black Forest Mountains, southwest Germany (48°01′ N, 7°58′ E). It ranges in altitude from 710 to 860 m a.s.l. with slopes of typically 20° and is covered with a dense natural stand of fully grown beech (*Fagus sylvatica*), fir (*Picea abies*) and spruce (*Abies alba*). The depth of the dominant Dystric Cambisol soil cover ranges from 1 m at the ridge top to 1·8 m on the lower slopes. With a high stone content of almost 50%, a soil texture of sandy loam and a porosity of 45% at the surface, the saturated hydraulic conductivity at 80 cm depth amounts to $0{\cdot}59 \times 10^{-2}$ m/s and increases to $1{\cdot}52 \times 10^{-2}$ m/s at the surface. At a soil depth between 80 cm and 120 cm a transition zone forms the interface between the soil layer and the periglacially formed talus parent material. The loose talus has a much higher permeability of approximately 8×10^{-2} m/s. Underlying bedrock is a dark paragneiss. The upper 4 m of the bedrock are intensively weathered, whereas below 5 m it is considered to be almost impermeable (von Wilpert *et al*., 1996). The valley floor of the stream draining the basin is covered by Quaternary gravel. Annual precipitation, predominantly rain, is 1400 mm. Throughfall depths in the hydrological winter half-year (517 mm), mainly caused by cyclonic precipitation events, slightly exceed those of the summer half-year (506 mm), when singular convective rainstorms prevail. Together with high evapotranspiration depths (588 mm) in the summer compared with winter (248 mm) this results in a distinct winter runoff of 444 mm, relative to the 141 mm in the hydrological summer half-year (von Wilpert *et al*., 1996).

Copyright © 2001 John Wiley & Sons, Ltd.

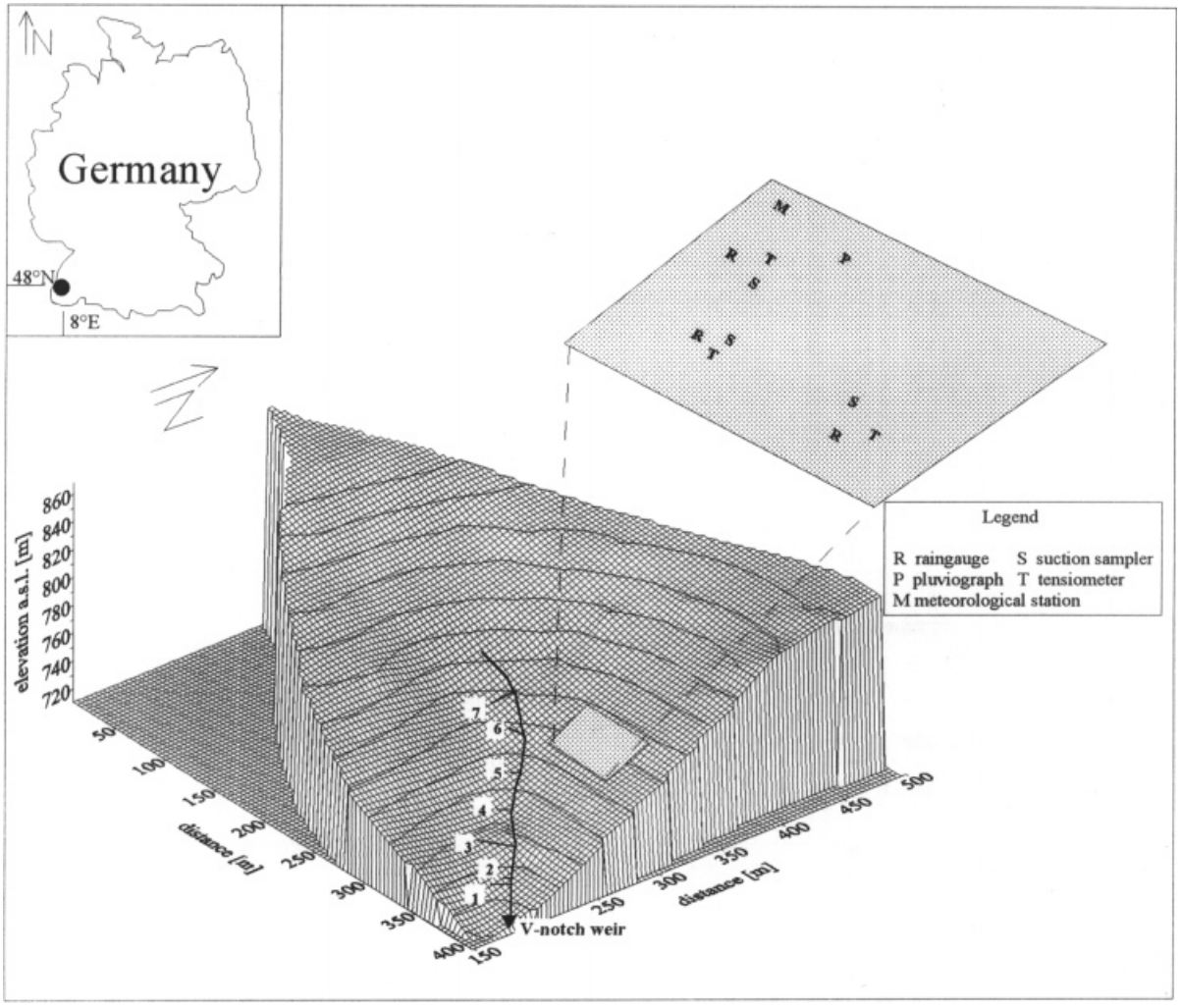

Figure 1. Maps showing location and topography of Conventwald catchment with instrumentation and assessed soil profile transects 1–7

METHODS

Recession analysis

Recession analysis of a hydrograph generally reveals information about the storage behaviour of a basin. Maillet's Law describes the depletion of a linear reservoir according to;

$$Q_t = Q_0 \times e^{-\alpha \times t} \ (L^3/T) \tag{1}$$

where Q_t is runoff at time t after Q_0, e is the Naperian base, and α is the recession coefficient, usually expressed in 1/day. The inverse value, expressed in days, represents the mean residence time of water in an idealized linear storage element with an outflow capacity close or equal to the represented storage system of the basin (cf. Toussaint, 1981). In this study recession coefficients are used for an estimated temporal subdivision of the total process of stormflow production. Recurring values are assumed to represent distinct system states of reservoir outflow (Tallaksen, 1995).

Copyright © 2001 John Wiley & Sons, Ltd.

Recession analyses of 35 recession limbs with a minimum length of 10 days after peak flow (Tallaksen, 1995) were carried out for the Conventwald basin by Pohl (1996) for the period 1 November 1991 to 1 July 1996 based on daily mean runoff (Table I). For each limb a semi-logarithmic plot was drawn, and straight lines were fitted starting from the second day after peak flow (Linsley *et al*., 1958). Owing to highly permeable soils and the absence of visible overland flow at the hillslopes, the influence of surface flow can be excluded after this 2-day interval.

To examine the actual system state with regard to long-term storage characteristics of the basin recession analyses were also conducted for storm events during the intensive measurement campaign (5 December 1996 to 10 March 1997).

Hydrometric data

Hydrometric data (throughfall intensity, matric potential of soil water and total discharge) were recorded at hourly intervals. Throughfall intensity was recorded with two 20°-inclined zinc gutters of 2 m^2 interception area, separately installed in the mixed stand. Both were connected to a joint tipping bucket by a flexible tube. At three soil depths (30 cm, 60 cm and 120 cm) matric potentials were determined by tensiometers about

Table I. Recession periods at the Conventwald basin 1 November 1991 to 1 July 1996 (after Pohl, 1996) (days counted from beginning of hydrologic year; $Q_{(p+2)}$ is discharge two days after peak flow)

Hydrological year (1 November to 31 October)	From (day)	To (day)	$Q_{(p+2)}$ [l/s]	α_2 [1/day]	α_1 [1/day]	$r^2\alpha_2$	$r^2\alpha_1$
92	22	41	3·5	0·16	0·10	0·906	0·971
92	69	76	6·9	0·15	0·06	0·998	0·964
92	188	207	2·7	0·15	0·07	0·954	0·994
93	37	45	7·0	0·20	0·08	0·996	0·990
93	59	72	2·6	0·16	0·06	0·989	0·948
93	162	170	1·9	0·15	0·07	0·991	0·981
93	209	217	0·9	0·16	0·05	0·982	0·896
93	238	247	0·7	0·14	0·07	0·993	0·961
94	2	10	1·4	0·15	0·06	0·983	0·993
94	77	85	7·0	0·18	0·09	0·987	0·963
94	90	113	5·2	0·13	0·05	0·991	0·995
94	121	131	4·6	0·10	0·05	0·962	0·951
94	170	184	4·5	0·13	0·05	0·998	0·966
94	211	220	3·8	0·12	0·05	0·987	0·945
94	243	261	2·8	0·15	0·04	0·979	0·983
94	267	282	0·6	0·11	0·06	0·978	0·994
94	338	353	0·8	0·11	0·05	0·991	0·966
95	42	56	6·1	0·21	0·09	0·982	0·985
95	64	72	4·1	0·15	0·08	0·955	0·987
95	89	100	7·3	0·21	0·09	0·993	0·984
95	112	133	8·1	0·17	0·06	0·996	0·985
95	185	193	2·7	0·18	0·09	0·987	0·959
95	245	253	0·8	0·15	0·04	0·910	0·959
95	269	279	0·7	0·12	0·06	0·998	0·995
95	335	358	3·4	0·14	0·07	0·996	0·992
96	26	47	6·2	0·16	0·05	0·994	0·966
96	66	76	3·1	0·19	0·07	0·988	0·991
96	217	232	6·1	0·2	0·07	0·908	0·953
Mean				0·16	0·07		
Standard deviation				0·029	0·016		
$t_{1/2}$ (days)				4·3	9·9		

Copyright © 2001 John Wiley & Sons, Ltd.

0·5–1·0 m away from the suction cups at the crown peripheries of the three dominating tree species. The crown peripheries had been identified as the hydraulically most relevant zones because of low root water uptake (von Wilpert and Mies, 1995). Total discharge was derived from a stage–discharge relationship at a V-notch weir.

Tracer application

Similar to other studies (e.g. Hooper and Shoemaker, 1986; Maule and Stein, 1990; Hildebrand *et al*., 1997; Hoeg *et al*., 2000) the environmental isotope oxygen-18 (^{18}O) and non-conservative dissolved silica (Si) served as indicators for the main runoff components. The ^{18}O component can be used to separate stormflow into event and pre-event components, whereas silica can be used to assess the flow paths that stormflow has followed. For the stable isotope ^{18}O, conservative behaviour along the flow paths can be presumed. In general, solely progressive mixing along flow paths occurs during the passage through the vadose and phreatic zones. With respect to input signals, this leads to a strongly attenuated and time-shifted tracer output function in runoff (cf. Lindenlaub, 1998). For dissolved silica, continuously increasing concentrations with increasing soil depth and contact time along the flow paths can be expected, as experimental studies in neighbouring basins confirm (Feger, 1993; Baur, 1994).

Based on ^{18}O and dissolved silica a preliminary end-member mixing analysis (Hooper *et al*., 1990) was carried out using mixing diagrams, which in addition to concentrations of total runoff comprised those of throughfall, soil waters (humus layer, 15 cm, 60 cm, 120 cm and 180 cm soil depth), and baseflow that represents groundwater. Mixing diagrams can provide an overview of the main differences of water sources present in a considered system and point to the required minimum number of sources needed to characterize the runoff response adequately. Tracer concentrations are assumed to be uniform in specific soil depths.

For the mixing model approach, equations equivalent to those used by Hinton *et al*. (1994) were applied, describing the mass balance for water, ^{18}O and dissolved silica, respectively:

$$Q_d = Q_t \times \frac{(c_t - c_{gw}) \times (\delta_{sw} - \delta_{gw}) - (\delta_t - \delta_{gw}) \times (c_{sw} - c_{gw})}{(c_d - c_{gw}) \times (\delta_{sw} - \delta_{gw}) - (\delta_d - \delta_{gw}) \times (c_{sw} - c_{gw})} \ (\mathrm{L}^3/\mathrm{T}) \tag{2}$$

$$Q_{sw} = Q_t \times \frac{(X_t - X_{gw})}{(X_{sw} - X_{gw})} - \frac{Q_d}{Q_t} \times \frac{(X_d - X_{gw})}{(X_{sw} - X_{gw})} \ (\mathrm{L}^3/\mathrm{T}) \tag{3}$$

$$Q_{gw} = Q_t \times \frac{(X_t - X_{sw})}{(X_{gw} - X_{sw})} - \frac{Q_d}{Q_t} \times \frac{(X_d - X_{sw})}{(X_{gw} - X_{sw})} \ (\mathrm{L}^3/\mathrm{T}) \tag{4}$$

Q is discharge, δ refers to ^{18}O content, c is concentration of dissolved silica, and the subscripts t, d, sw and gw refer to total runoff, direct runoff, and contributions from soil and groundwater, respectively. In Equations 3 and 4 variable X optionally refers either to the concentration of dissolved silica or to the respective ^{18}O content. The combination of Equations 2–4 yields the three unknown runoff components Q_d, Q_{sw} and Q_{gw}.

To apply the mixing model to total runoff, Q_t at time t and the initial tracer concentrations of the individual components have to be known and were taken from the mixing diagrams. Tracer concentrations of all reservoirs involved are assumed to be constant over the course of the storm event (e.g. Sklash and Farvolden, 1979), although changes in tracer content during a storm event have been proven experimentally for another basin (Buttle and Peters, 1997). The validity of the assumption of non-time-variant end-members could not be investigated separately within this study. Non-time-variant end-members have been used in many other studies (e.g. Maule and Stein, 1990; Hoeg *et al*., 2000).

In addition to oxygen-18 (^{18}O) and dissolved silica (Si), the additional natural tracers potassium (K), dissolved organic carbon (DOC), and sulphate (SO_4) were measured in the soil waters and in runoff to obtain further information about flow paths and the location of runoff sources.

Potassium (K) is derived mainly from leaching in the forest canopy and the organic matter of the upper soil zone. Fast sorption by ion exchange processes is assumed in the soil matrix at K-specific exchange sites

Copyright © 2001 John Wiley & Sons, Ltd.

of the vermiculite clay minerals. Potassium is expected to label predominantly throughfall and surface runoff (Elsenbeer *et al*., 1994). Dissolved organic carbon (DOC) is assumed to label water derived from organic soil horizons. Being highly sorptive its occurrence in stream flow points to direct runoff components, such as overland flow and water bypassing the immobilizing soil matrix via preferential flow paths (Jardine *et al*., 1990). Sulphate (SO_4) predominantly occurs as a weathering product of the underlying gneiss, and is therefore assumed to label the water that passed the deeper mineral soil (1 m to 1·8 m), where it might be stored as remobilizable, amorphous jurbanite ($AlOHSO_4$) (von Wilpert *et al*., 1996).

Assessment of hydrochemical data

During the measurement campaign, which ran from 5 December 1996 to 10 March 1997, throughfall was collected in three rain gauges, each situated underneath one of the three dominating tree species, and sampled every 3–4 days (Figure 1). Soil water was extracted by suction cups at the crown peripheries of the three dominating tree species at five different depths: (i) humus layer and 15 cm soil depth, hereafter referred to as 'topsoil'; (ii) 60 cm soil depth, representing the 'upper profile'; (iii) 120 cm and 180 cm soil depth, hereafter referred to as 'subsoil'. Suction of 30 kPa was exerted every 8 h for 15 min. Aliquots were sampled at two-weekly intervals. Tracer contents of soil waters and throughfall were weighed according to the percentage areal coverage of the respective tree species to account for species distribution. Basin discharge was sampled hourly at the outlet using an automatic sampler.

Filtered water samples were analysed for ^{18}O by mass spectrometry ('Delta S', Finnigan Mat) with an accurracy of ±0·15‰. Silica concentrations were obtained by spectrophotometry ('Spectronic 1001 Plus', Milton Roy) as were the DOC contents ('Autoanalyzer', Skalar), both with an accurracy of ±0·1 mg/l. Potassium was analysed by flame photometry ('Spectroflame', Spectro) with an accurracy of ±0·3 mg/l, and SO_4 concentrations were obtained by ion chromatography ('DX-100 Ion Chromatograph', Dionex) with an accurracy of ±0·2 mg/l.

Soil survey

Thirty soil profiles of 1 m depth from seven transects orientated perpendicularly to the draining channel at the bottom of the western hillslope (Figure 1) were analysed for redoximorphic features (I. Haag and Forest Research Institute, unpublished data, 1994). These should provide further information about soil hydrological processes.

RESULTS AND DISCUSSION

Five storm events (A–E) of different magnitude and duration can be delimited during the period of intensive investigation (5 December 1996 to 10 March 1997) of the runoff response of the Conventwald basin (Figure 2). Only the small events B and D could be assessed completely by the tracer approach and will be analysed later.

Recession analysis

Long-term recession analyses by Pohl (1996), which are compiled in Table I, as well as recession analyses of the events A and C together with their respective actual regression coefficients (Figure 3a and b) provide a general picture of two distinct phases in recession response that reflects the following pattern: a fast reacting 'reservoir' with a mean recession coefficient of $\alpha_2 = -0{\cdot}16$ 1/day represents the first phase starting with the abating of surface flow, which is followed by a delayed reacting 'reservoir' with $\alpha_1 = -0{\cdot}07$ 1/day, representing the second phase of event-related runoff with slower response.

Both recession phases, α_2 more distinct than α_1, indicate weak positive trends between the recession coefficient and the amount of discharge two days after peak flow ($Q_{(p+2)}$) (Figure 4). Seasonal effects for the

Copyright © 2001 John Wiley & Sons, Ltd.

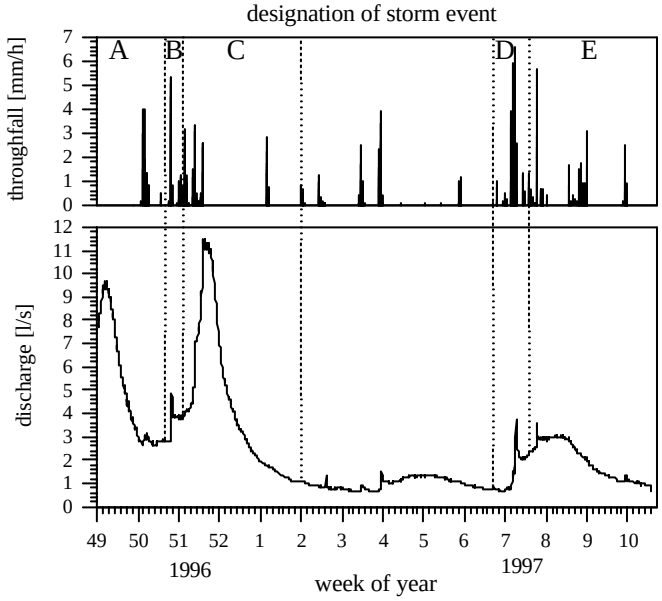

Figure 2. Throughfall (bars), runoff (line), and designation of assessed storm events A to E of the measurement period (5 December 1996 to 10 March 1997)

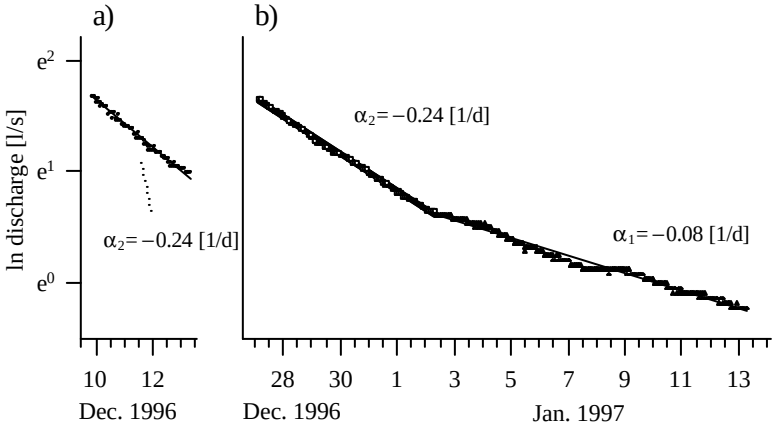

Figure 3. Recession analyses of preceeding storm hydrograph (a) A and (b) C

observed scattering of recession coefficients due to evapotranspiration (Zecharias and Brutsaert, 1988) could not be established (see Table I), as the influence of vegetation seems to be small compared with soil and aquifer characteristics. Also spatial variabilities in rain storm patterns causing differences in the distribution of flow paths, which are rendered problematic for large basins (Laurenson, 1961), should not apply for the small Conventwald basin.

As suggested by the long-term recession analyses (Table I) the latter stages of the hydrograph response at the Conventwald basin can be characterized by the two main flow systems or two storage components involved. Each can be viewed as representing a certain system state, which is analysed in more detail in the following sections together with tracer and matric potential data.

Copyright © 2001 John Wiley & Sons, Ltd.

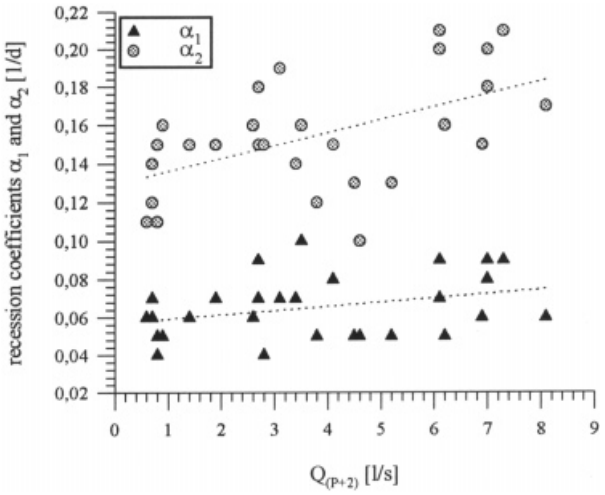

Figure 4. Recession coefficients (after Pohl, 1996) as a function of discharge two days after peak flow

Hydrometric data

Throughfall and discharge of storm events B and D, respectively (Figure 5a and b), served to calculate a simple water balance by determining runoff coefficients (i.e. throughfall versus peak flow ratios). Both events exhibit relatively small values in the range 0·02–0·04, which are typical for runoff behaviour in basins with highly permeable soils over crystalline bedrock (Feger, 1993). Nevertheless, the runoff coefficients are highly variable within the single events. When dividing event D into the three distinct subevents 1, 2 and 3, the coefficients show an increase from 0·0035 (1) and 0·0072 (2) up to 0·036 (3) (Figure 5b). Storage at the ground surface and in the unsaturated zone and the increasing recharge of water into the hillslope aquifer during the series of subevents may contribute to such low runoff coefficients. Downward propagation of the infiltration front initiated by individual precipitation events is illustrated for storm events B and D by the course of soil water matric potentials at three depths (30 cm, 60 cm and 120 cm) (Figure 5a and b). These are assumed to be distributed uniformly over the basin investigated, neglecting spatial irregularities as reported for macroporous forest soils (e.g. Wilson *et al*., 1990). Very low matric potentials at 30 cm soil depth can be attributed to root water uptake by the conifers, the effect of which seems to be diminished in 60 cm and 120 cm soil depth.

Rapid changes of matric potential at a single soil depth suggest a displacement velocity of the infiltration front of several decimetres per day. Therefore, more than one day is required for water of a precipitation event to pass the unsaturated zone, which at the hillslopes is about 120 cm thick, suggested by low matric potentials at that depth (Figures 1, 5a and b). In contrast, the hydrographs show maximum runoff just a few hours after the precipitation events have ceased (Figure 5a and b). For both events investigated the occurrence of maximum runoff is synchronized with the infiltration fronts reaching the 60 cm level at the hillslopes. Apparently, for both events, the hillslopes do not contribute significantly to the fast and event related peak flow. Alternatively, a contribution of the hillslopes to the baseflow system can be hypothesized.

The tracer approach: mixing analysis and hydrograph separation

Soil waters prior to event B show a general tendency towards enrichment of ^{18}O with increasing depth (Figure 6a).

Prior to event D vertical ^{18}O distribution shows depletion towards 60 cm depth followed by enrichment downward from 60 cm to 180 cm soil depth (Figure 6a). Despite the principal tendency of progressive mixing along the flow path through the soil, enriched water from the actual precipitation event seems to prevail in the

Copyright © 2001 John Wiley & Sons, Ltd.

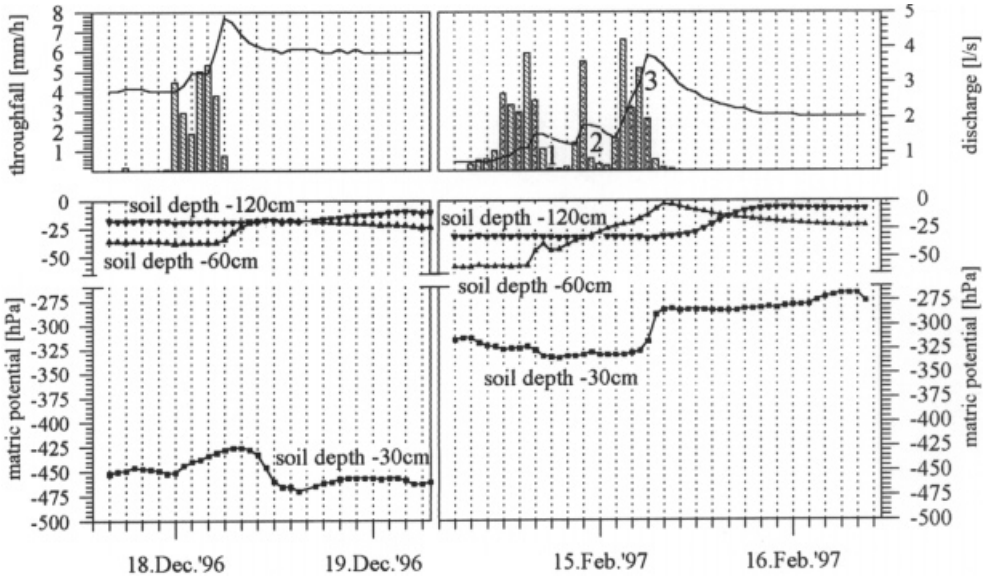

Figure 5. Throughfall, total runoff and matric potentials of three soil depths during (a) event B and (b) event D

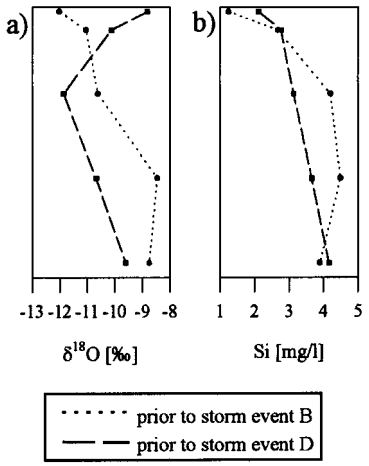

Figure 6. Vertical tracer distribution within soil profiles prior to storm event B and D of (a) ^{18}O and (b) dissolved silica

upper few centimeters of the profile, whereas not far beneath (60 cm level) it is dominated by depleted water of the preceding precipitation event. With increasing depth the reverse tendency towards more enriched isotope values occurs again, presumably as a result of former precipitation events of even higher ^{18}O enrichment. Soil waters of both events (Figure 6a) illustrate that ^{18}O contents of the unsaturated zone of a basin are in a continuously changing and dynamic state (McDonnell *et al*., 1991). Consequently, the antecedent conditions have to be considered.

A positive relationship between increasing dissolved silica concentration and increasing soil depth is observed (Figure 6b) allowing clear designation of Si labelled waters. Thus, dissolved silica is suitable for our purpose to identify specific soil depths as potential runoff sources.

Copyright © 2001 John Wiley & Sons, Ltd.

The mixing diagram for event B (Figure 7a) exhibits a depletion in ^{18}O content of total runoff relative to waters of the subsoil (120 cm and 180 cm depth) and enrichment compared with soil waters of the upper profile (60 cm depth) and the topsoil (15 cm depth and humus layer), and throughfall. In contrast to event B, where stormflow was triggered by relatively depleted throughfall ($\delta^{18}O = -11{\cdot}98‰$), event D is initated by throughfall with a 'heavy' ^{18}O signature ($\delta^{18}O = -7{\cdot}1‰$) (Figure 7b). The ^{18}O contents of total runoff are lower compared with those of throughfall and water from the humus layer, and higher relative to soil waters from the upper profile (60 cm depth) and the subsoil (120 cm and 180 cm depth).

For both storm investigated events the dissolved silica concentrations of total runoff are higher than those of the evaluated soil depths and almost coincide with those of baseflows (Figure 7b). Therefore, we assume that most of the water has to pass through the whole soil profile (Figure 6b) to accumulate dissolved silica before it reaches the channel system, although other studies point out a significant acquisition of dissolved silica by event water on its passage through a drainage basin (e.g. Kennedy, 1971; Shimada *et al*., 1993; Buttle and Peters, 1997).

To designate total runoff of the Conventwald basin for events B and D to specific source areas the mixing diagrams (Figure 7a and b) suggest three end-members. Two system states of delayed reservoir outflow in the basin (Table I; Figure 3a and b) confirm a contribution of two runoff components. A third reservoir with immediate outflow (cf. Duysings *et al*., 1983) might be disregarded as a result of the $Q_{(p+2)}$ criterion of recession analysis. Pohl (1996), who tested a two-component model for five stormflow events at the Conventwald basin, also recommends the separation into three runoff components.

For event B, the maximum tracer concentrations occurring in runoff can be explained best by the water sources from the upper profile (60 cm soil depth) as the third end-member in addition to throughfall and baseflow (Figure 7a). However, for storm event D alternatives in selecting the third end-member were possible, which could involve concentrations at the upper profile (60 cm) as well as at the subsoil (120 cm or 180 cm depth) (Figure 7b). For reasons of comparability, also the upper profile (60 cm depth) was chosen as a source of the soil water component, in addition to baseflow and water of the 'new' event, i.e. throughfall.

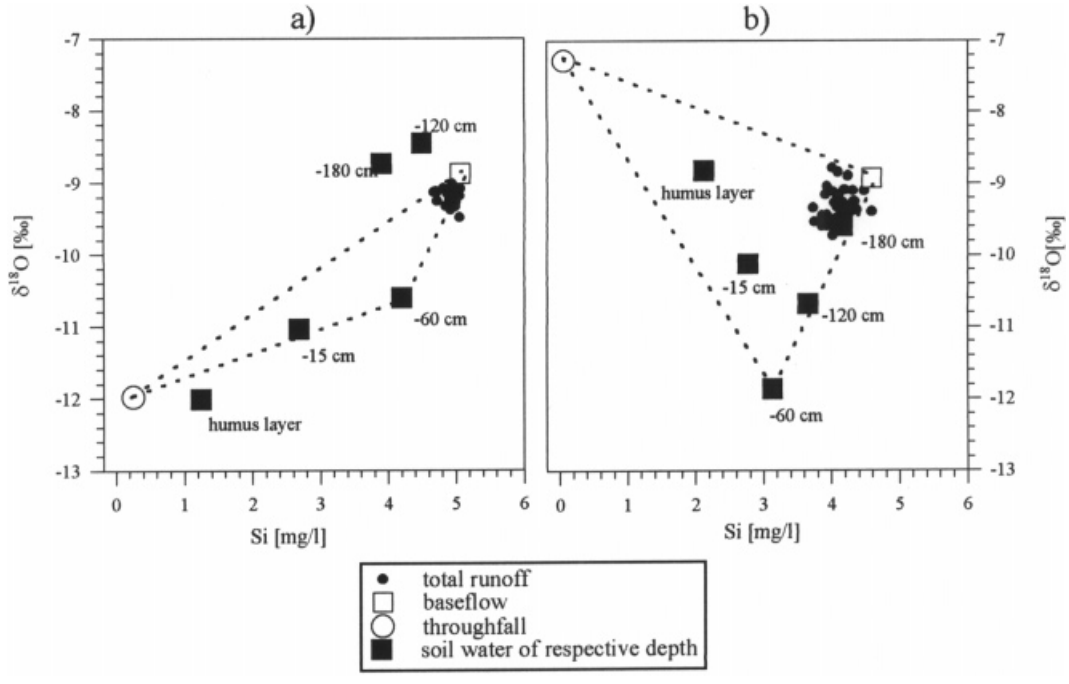

Figure 7. Mixing diagram comprising throughfall, baseflow and soil waters prior to (a) storm event B and (b) storm event D

Copyright © 2001 John Wiley & Sons, Ltd.

Considering the tracer behaviour of total runoff during the course of both events, dissolved silica follows a general pattern familiar from other studies (Hooper and Shoemaker, 1986; Hildebrand *et al*., 1997), where throughfall input causes a dilution effect, based on mixing of silica-rich water of the 'old' baseflow component with 'new' water of shorter residence time and a low Si concentration (Figure 8a and b).

The situation in runoff concerning ^{18}O is more complex, owing to its irregular vertical distribution in the soil profile (Figure 6a). Although event B is initiated by a depleted throughfall event (−11·98‰) the ^{18}O content in runoff persists at a rather enriched level (Figure 8a). It thus appears that isotopically 'heavy' water within the deeper soil zones, as illustrated in the mixing diagram (Figure 7a), is displaced during the event. Here, an isotopic effect in runoff is probably caused by a relatively small antecedent precipitation event 5–7 hours prior to the actual event B (see Figure 5a).

Similarly, despite being initiated by relatively enriched throughfall (−7·28‰), tracer contents of runoff during event D tend to isotopically 'lighter' ^{18}O values after peak flow (Figure 8b). Again, an explanation can be provided with reference to the mixing diagram (Figure 7b), where the dominance of depleted water in deeper soil layers is exhibited.

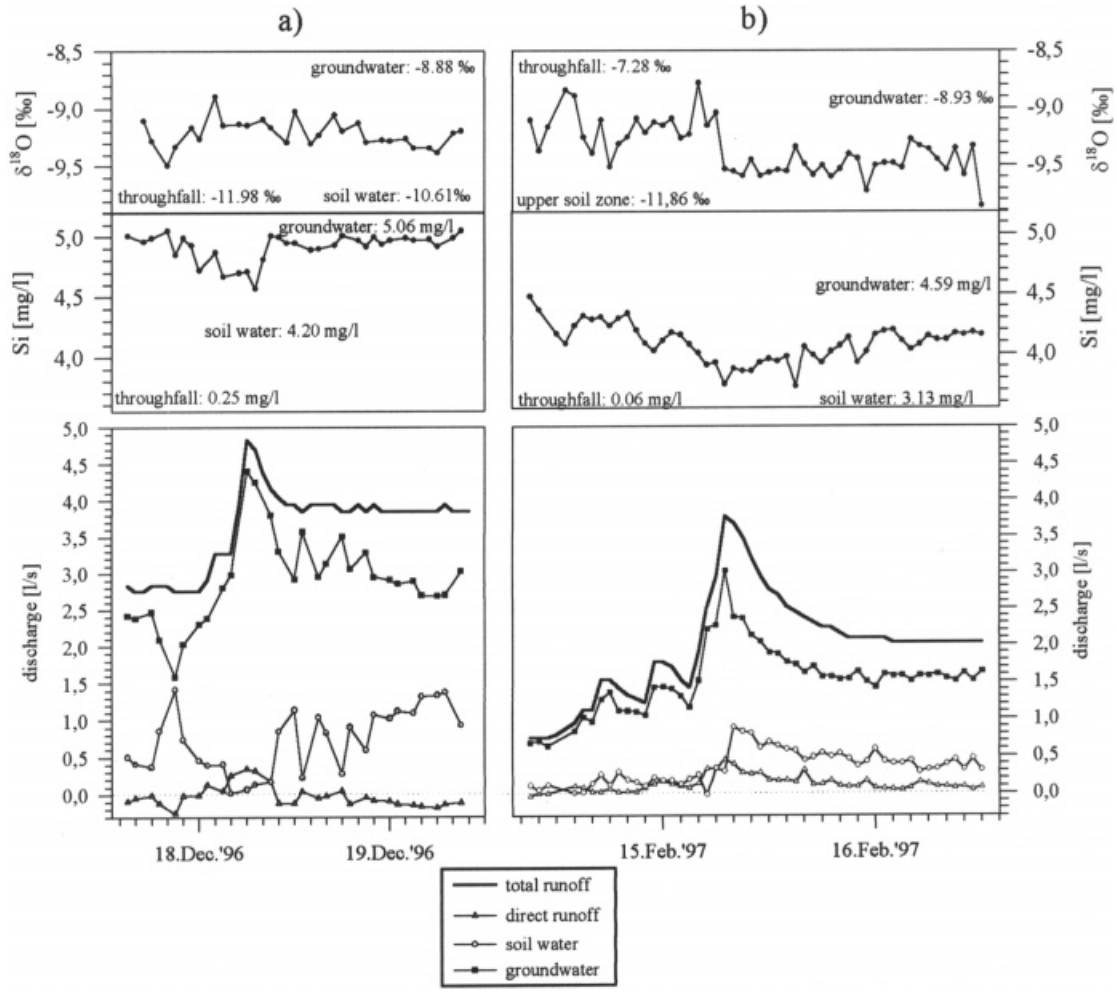

Figure 8. Chemographs of ^{18}O and dissolved silica and three-component hydrograph separation for (a) storm event B and (b) storm event D

Copyright © 2001 John Wiley & Sons, Ltd.

Inserting dissolved silica and ^{18}O values of the source components throughfall, soil water from the upper profile (60 cm depth), and baseflow together with tracer concentrations of total runoff into the three-component mixing model (Equations 2–4) reveals status and temporal occurrence of the three runoff components direct runoff, soil water and groundwater.

As indicated by a small participation of direct runoff at stormflow (Figure 8a and b) the impact of the tracer content of throughfall (event water) on runoff is very small for both events. Participation of direct runoff at stormflow B is very low and even becomes negative at times (Figure 8a). This unrealistic finding might point to a two-component stormflow generation pattern for event B, because no clear fluctuations in isotopic composition of streamwater occurred during the event. Missing isotopic evidence of rainfall input in runoff is also reported for several stormflow situations of a nearby basin (Neal *et al*., 1997), where a contribution of direct rainfall to stream stormflow is questioned. Moreover, the actual recession analysis of the preceding event A (Figure 3a) displays an incomplete depletion of the 'fast reacting reservoir'. Thus, at the beginning of storm event B, true 'baseflow conditions' hardly existed. Total runoff of storm event B therefore was composed completety of soil water and groundwater, i.e. of outflowing reservoirs, with direct runoff being negligible. In contrast to event B, event D displays a clear direct runoff component restricted to a time period during peak flow with increasing significance from subevent to subevent.

The soil water component of the Conventwald basin displays a delayed occurrence in total runoff with respect to groundwater. At both events the rising limbs of the soil water runoff fractions appear after peak flow of total runoff. Together with the small direct runoff component this implies that the steep rise in total runoff is attributed mainly to the groundwater component. Consequently, a mechanism for runoff production has to exist, where the actual precipitation activates the groundwater reservoir prior to the occurrence of the soil water component in the channel system.

Additional tracers investigated

Prior to both storm events studied, DOC and K show increased concentrations in the topsoil (15 cm depth and humus layer) (Figure 9a and b). In contrast to its general vertical distribution, here the SO_4 content in the greatest soil depth (180 cm) appears to be relatively small. In the soil matrix, distinct SO_4 accumulations were found in the subsoil around 120 cm depth (Figure 9c), which probably is adsorbed sulphate formerly deposited from air pollutants (von Wilpert *et al.* 1996).

As a result of the unambiguous designation of stormflow runoff components further examinations are restricted to storm event D.

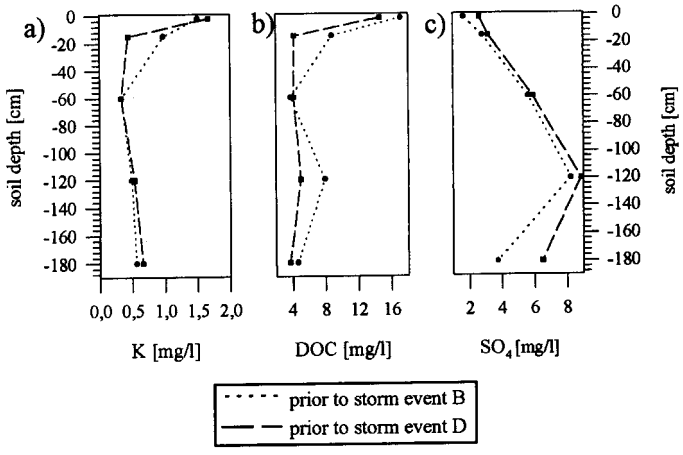

Figure 9. Vertical tracer distribution within soil profiles prior to storm event B and D of (a) K, (b) DOC and (c) SO_4

Copyright © 2001 John Wiley & Sons, Ltd.

In the total runoff of storm event D smaller DOC peaks occur together with precipitation events, whereas the position of the major peak coincides with soil water contribution to runoff (Figures 8b and 10). These temporal distributions of the DOC concentration suggest fast infiltration processes via macropores, as reported for this headwater catchment by Brodersen *et al*. (2000), as well as flow along bedrock outcrops in the near-channel area of the basin. The time delay of the major DOC peak probably reflects the time lag between effective precipitation and the onset of the stand's stemflow, which displaces DOC-rich waters of the topsoil via macropores, e.g. root channels, towards the stream.

Concerning the K concentration of total runoff, the second, smaller peak also might be attributed to delayed stemflow. In the Conventwald basin K concentrations of stemflow have been found to exceed that of canopy throughfall by up to one order of magnitude (von Wilpert *et al*., 1996). The maximum K concentration at peak flow of event D might label overland flow processes of the direct runoff component (Figures 8b and 10).

The concentration minima in SO_4 (Figure 10) are explicable as a 'dilution effect', analogous to dissolved silica (Figure 8b), caused by soil water reaching the stream from upper soil layers.

Soil survey

Redoximorphic features occurred as horizons of approximately 15 cm thickness. A corresponding depth interval can be interpreted as transiently saturated, or 'tension-saturated' with reference to Freeze and Cherry (1979). Averaged for the seven transects, the vertical distance between the redoximorphic horizon and the ground surface increased upslope by 10 cm/m, pointing to the downslope convergence of flow (Dunne, 1978).

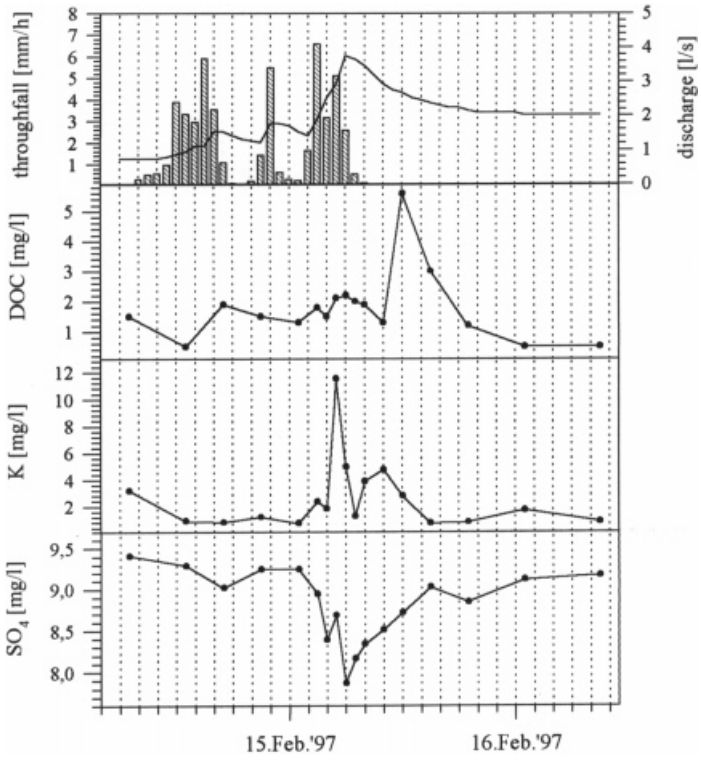

Figure 10. Chemographs of DOC, K and SO_4 during storm event D

Copyright © 2001 John Wiley & Sons, Ltd.

Integrated conceptual model of stormflow and runoff generation

Based on the results presented so far, a coherent picture of stormflow mechanisms at the Conventwald basin can be drawn. This relies on two *structural* units:

(1) a near-channel reservoir, controlling the release of water during the event via its hydraulic potential;
(2) a hillslope aquifer, serving predominantly as a baseflow recharge system (Figure 11).

Dry antecedent conditions may restrain the near-channel area of fast runoff production to the valley floors. This area expands upslope under wet conditions, which may favour an intensified displacement and release of soil water, because the hydraulic dynamics of the hillslope aquifer are most developed at a high degree of saturation.

Temporally the event-related runoff production is divisible into three steps, according to the recession analyses, the occurrence of distinct components in runoff and the chemographs.

Stage 1. Stage 1 (Figure 11), comprises the period between the fast and steep rise of the hydrograph and peak flow. Saturation overland flow (Dunne, 1978) from limited areas on the valley floors is assumed to be the initiating mechanism. Contribution of the direct runoff component to total stormflow runoff is supported by the characteristic 'event' related (i.e. isotopic signature similar to throughfall) isotope values (Figure 8b) as well as by the potassium peak at the beginning of event D (Figure 10).

The second main flow component during the first section of stormflow generation is 'old' water, characterized by high dissolved silica concentrations and a smoothed variation in ^{18}O content (Figure 8b). Because of its fast release, water contribution from a near-channel reservoir within the basin is supposed, situated in the Quaternary gravel of the valley bottom. To explain the steep rise of the hydrograph a rapid change in the hydraulic conditions inside this reservoir must occur. Similar phenomena were described as groundwater ridging (Sklash and Farvolden, 1979), assuming a distinct capillary fringe, which unlikely exists in the coarse gravel of the Conventwald basin's valley floor. McGlynn *et al.* (1999) experimentally demonstrated

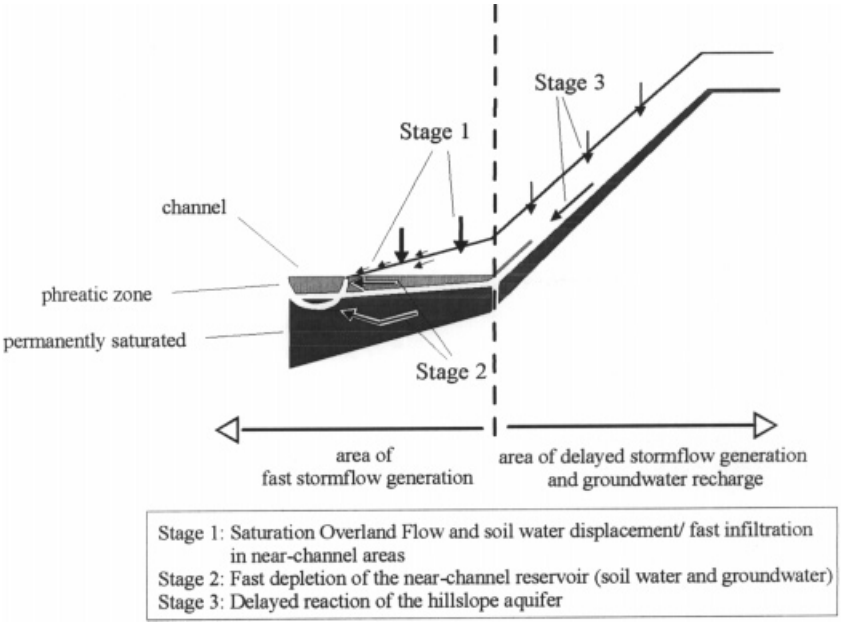

Figure 11. Conceptual model of stormflow generation at a hillslope segment

Copyright © 2001 John Wiley & Sons, Ltd.

strong upward discharge gradients at the near-channel riparian zone during snowmelt in a temperate headwater catchment, referred to as 'transmissivity feedback' (Bishop, 1991). A similar mechanism could be envisaged for the drastic change of hydraulic conditions in the near-channel area of the Conventwald basin. The thickness of redoximorphic soil horizons might indicate the vertical zone involved in transmissivity feedback during stormflow situations.

As one initiating mechanism for an instant replenishment of the near-channel reservoir, fast infiltration along macropores is conceivable, as suggested by distinct shifts of DOC concentration (Figure 10) in total runoff (Peters *et al*., 1995). A second probable mechanism is the displacement of water of the unsaturated soil zone by infiltrating precipitation. In view of the downslope-decreasing vertical distance of redoximorphic horizons to the ground surface, a high degree of saturation in the near-channel area can be expressed. Supplemented by sufficiently intensive throughfall events this combination may lead to a drastic increase in transmissivity as the saturated zone thickens, resulting in a fast mobilization and displacement of soil water (McGlynn *et al*., 1999). This first has to pass the near-channel reservoir before being released to runoff, and therefore does not occur in the basin outflow until the recession limb of the hydrograph (Figure 8b). For a single precipitation–runoff event the hillslopes are unlikely to contribute significantly to the system response beyond their pre-event status, according to the hydrometric data (Figure 5b) and the very low runoff coefficients (see 'Hydrometric data').

Stage 2. Stage 2 of stormflow generation (Figure 11) comprises peak flow and the subsequent fast depletion of the near-channel reservoir. Direct runoff abates within the first or second day after precipitation has ceased (Figure 8b). Afterwards the reservoir outflow tends towards the average discharge, expressed by a recurring recession coefficient with a $t_{1/2}$ of 4·3 days (Table I). Total runoff then consists mainly of soil water supplemented by the groundwater component. The isotopic signature of total runoff does not yet indicate a thorough mixing with groundwater, which entered the system formerly (Figure 8b). This isotopic pattern of total runoff is reflected by low concentrations of the geochemicals dissolved silica and sulphate (Figures 8b and 10), a finding also reported from other basins (Hooper and Shoemaker, 1986; Hildebrand *et al*., 1997).

Because of a relatively slow water transfer from the hillslopes to the fast depleting groundwater reservoir, the hillslopes are assumed still not to contribute significantly to the system response during stage 2. Despite the integrated nature of hillslope–floodplain systems (Dunne, 1978), specific changes in tracer concentrations and recession characteristics provide a reason for segregating a third stage in the stormflow generation process.

Stage 3. The third stage (Figure 11) of stormflow generation is characterized by a stable contribution of the soil water component (Figure 8b) and might be initiated by an abrupt drop of the hydraulic potential at the near-channel reservoir. Recession analyses show a clear and recurring point of transition towards a second characteristic reservoir outflow with an average $t_{1/2}$ of 9·9 days (Table I). This transition point presumably indicates the gradual onset of the hillslope aquifer's system response, resulting in a higher flow activity at the soil–bedrock interface. Dissolved silica and sulphate in total runoff reach levels close to the pre-event status (Figures 8b and 10), while isotope values still point to the contribution of soil water (Figure 8b).

The third stage of stormflow generation, therefore, is characterized basically by an increased recharge activity of the hillslope aquifer towards the groundwater reservoir.

CONCLUSIONS

The assessment of the behaviour of selected natural tracers allows a consistent reconstruction of those mechanisms that are responsible for stormflow generation at the Conventwald basin. Stormflow supposedly is generated by rapidly responding groundwater, which is augmented by other mechanisms such as runoff from saturated areas. These qualitative results were quantified by separating the hydrograph into three components, i.e. direct runoff, soil water and groundwater. Analysed stormflow events of similar discharge pointed to two

Copyright © 2001 John Wiley & Sons, Ltd.

different sections of the basin: the near-channel area, basically responsible for the instant water supply of stormflow runoff, and the hillslopes. The temporal process of stormflow generation is divisible into three stages with different contributions of the single runoff components and source areas:

(1) A rapid release of water by soil water displacement/fast infiltration at the near-channel area, supplemented by saturation overland flow;
(2) fast depletion of the near-channel reservoir comprising soil water and groundwater;
(3) delayed reaction of the hillslope aquifer.

These findings were supported by hydrometric data and, additionally to previous studies, extensive recession analyses. Incorporation of recession analysis to evaluate the significance of single source components in subsequent stormflow events is demonstrated to be a useful addition in the spatio-temporal interpretation of hydrographs and stormflow generation. Definition of representative source components of an individual storm event is strongly related to antecedent conditions as well as to the spatial discretization of sampling devices, particularly in the soil zone.

REFERENCES

Baur S. 1994. *Anwendung hydrochemischer Modelle zur Erklärung der Aluminium-Dynamik im Stoffumsatz von Waldökosystemen des Südschwarzwalds*. PhD thesis, University Freiburg.

Bazemore DE, Eshleman KN, Hollenbeck KJ. 1994. The role of soil water in stormflow generation in a forested headwater catchment: synthesis of natural tracer and hydrometric evidence. *Journal of Hydrology* **162**: 47–75.

Bishop KH. 1991. *Episodic increases in stream acidity, catchment flow pathways and hydrograph separation*. PhD thesis, University of Cambridge, Department of Geography, 246 pp.

Brodersen C, Pohl S, Lindenlaub M, Leibundgut Ch, von Wilpert K. 2000. Influence of vegetation structure on isotope content of throughfall and soil water. *Hydrological Processes* **14**: 1439–1448.

Burns DA, Hooper RP, McDonnell JJ, Freer JE, Kendall C, Beven K. 1998. Base cation concentrations in subsurface flow from a forested hillslope: the role of flushing frequency. *Water Resources Research* **34**: 3535–3544.

Buttle JM, Peters DL. 1997. Inferring hydrological processes in a temperate basin using isotopic and geochemical hydrograph separation: a re-evaluation. *Hydrological Processes* **11**: 557–573.

Dunne T. 1978. Field studies of hillslope flow processes. In *Hillslope Hydrology*, Kirkby M (ed.). Wiley: Chichester; 256–293.

Duysings JJHM, Verstraten JM, Bruynzeel L. 1983. The identification of runoff sources of a forested lowland catchment: a chemical and statistical approach. *Journal of Hydrology* **64**: 357–375.

Elsenbeer H, West A, Bonell M. 1994. Hydrologic pathways and stormflow hydrochemistry at South Creek, northeast Queensland. *Journal of Hydrology* **162**: 1–21.

Feger KH. 1993. Bedeutung von ökosysteminternen Umsätzen und Nutzungseingriffen für den Stoffhaushalt von Waldlandschaften. *Freiburger Bodenkundliche Abhandlungen H* **31**: 257 pp.

Freeze RA, Cherry JA. 1979. *Groundwater*. Prentice-Hall: Englewood Cliffs, NJ; 604 pp.

Güntner A, Uhlenbrook S, Seibert J, Leibundgut Ch. 1999. Multi-criterial validation of TOPMODEL in a mountainous catchment. *Hydrological Processes* **13**: 1603–1620.

Harris DM, McDonnell JJ, Rodhe A. 1995. Hydrograph separation using continuous open system isotope mixing. *Water Resources Research* **31**: 157–171.

Havel M, Peters NE, Cerny J. 1999. Longitudinal patterns of stream chemistry in a catchment with forest dieback, Czech Republic. *Environmental Pollution* **104**: 157–167.

Hildebrand AC, Lindenlaub M, Leibundgut Ch. 1997. Behaviour and comparison of dissolved silica and oxygen-18 as natural tracers during snowmelt. In *Tracer Hydrology. 7th International Symposium on Water Tracing*, Kranjc A (ed.). AA Balkema: Rotterdam; 161–166.

Hinton MJ, Schiff SL, English MC. 1994. Examining the contributions of glacial till water to storm runoff using two- and three-component hydrograph separation. *Water Resources Research* **30**: 983–993.

Hoeg S, Uhlenbrook S, Leibundgut Ch. 2000. Hydrograph separation in a mountainous catchment — combining hydrochemical and isotopic tracers. *Hydrological Processes* **14**: 1199–1216.

Hooper RP, Shoemaker C. 1986. A comparison of chemical and isotopic hydrograph separation. *Water Resources Research* **22**: 1444–1454.

Hooper RP, Christophersen N, Peters NE. 1990. Modelling streamwater chemistry as a mixture of soilwater end-members — An application to the Panola Mountain catchment, Georgia, USA. *Journal of Hydrology* **116**: 321–343.

Jardine PM, Wilson GV, McCarthy JF, Luxmoore RJ, Taylor DL, Zelazny LW. 1990. Hydrogeochemical processes controlling the transport of dissolved organic carbon through a forested hillslope. *Journal of Contaminant Hydrology* **6**: 3–19.

Jayatilaka CJ, Gillham RW. 1996. A deterministic-empirical model of the effect of the capillary-fringe on near-stream area runoff. 1. Description of the model. *Journal of Hydrology* **207**: 299–315.

Jenkins A, Ferrier RC, Harriman R, Ogunkoya YO. 1994. A case study in hydrochemistry: conflicting interpretations from hydrological and chemical observations. *Hydrological Processes* **8**: 335–349.

Copyright © 2001 John Wiley & Sons, Ltd.

Kendall C, McDonnell JJ (eds.) 1998. *Isotope tracers in catchment hydrology*. Elsevier: Amsterdam.
Kennedy VC. 1971. Nonequilibrium systems in natural water chemistry. *Advances in Chemistry Series* **106**: 94–130.
Laurenson BE. 1961. A study of hydrograph recession curves of an experimental catchment. *Journal of Institute Engineers, Australia* **33**: 253–258.
Lindenlaub M. 1998. *Abflußkomponenten und Herkunftsräume im Einzugsgebiet der Brugga: Aspekte zeitlicher und räumlicher Skalierung*. PhD thesis, University of Freiburg.
Linsley RK, Kohler MA, Paulhus JLH, 1958. Hydrograph analysis. *Hydrology for Engineers*. McGraw-Hill: New York.
Maule CP, Stein J. 1990. Hydrologic flow path definition and partitioning of spring meltwater. *Water Resources Research* **26**: 2959–2970.
McDonnell JJ. 1990. A rationale for old-water discharge through macropores in a steep, humid catchment. *Water Resources Research* **26**: 2821–2832.
McDonnell JJ, Stewart MK, Owens JF. 1991. Effect of catchment-scale subsurface mixing on stream isotopic response. *Water Resources Research* **27**: 3065–3073.
McGlynn BL, McDonnell JJ, Shanley JB, Kendall C. 1999. Riparian zone flowpath dynamics during snowmelt in a small headwater catchment. *Journal of Hydrology* **222**: 75–92.
McNamara J, Kane D, Hinzman L. 1997. Hydrograph separations in an Arctic watershed using mixing model and graphical techniques. *Water Resources Research* **33**: 1707–1719.
Neal M, Neal C, Brahmer G. 1997. Stable oxygen isotope variations in rain, snow and streamwaters at the Schluchsee and Villingen sites in the Black Forest, SW Germany. *Journal of Hydrology* **190**: 102–110.
Peters D, Buttle J, Taylor C, LaZerte B. 1995. Runoff generation in a forested, shallow soil, Canadian Shield basin. *Water Resources Research* **31**: 1291–1304.
Pohl S. 1996. *Abflußbildung im Einzugsgebiet 'Conventwald' auf der Grundlage von Ganglinienanalyse und Isotopenuntersuchungen.* MSc thesis, Institute of Hydrology, University of Freiburg.
Rice KC, Hornberger GM. 1998. Comparison of hydrochemical tracers to estimate source contributions to peak flow in a small, forested, headwater catchment. *Water Resources Research* **34**: 1755–1766.
Shimada Y, Ohte N, Tokuchi N, Suzuki M. 1993. A dissolved silica budget for a temperate forested basin. *International Association of Hydrological Sciences Publication* **215**: 79–88.
Sklash MG, Farvolden RN. 1979. The role of groundwater in storm runoff. *Journal of Hydrology* **43**: 45–65.
Sklash MG, Stewart MK, Pearce AJ. 1986. Storm runoff generation in humid headwater catchments. 2. A case study of hillslope and low-order stream response. *Water Resources Research* **22**: 1273–1282.
Tallaksen LM. 1995. A review of baseflow recession. *Journal of Hydrology* **165**: 349–370.
Toussaint B. 1981. Ermittlung der Leerlaufkoeffizienten nach Maillet und des effektiv nutzbaren Gesteinsvolumens in hessischen Flußgebieten durch Auswertung der Abflüsse im Trockenjahr 1976. *Deutsche Gewässerkundliche Mitteilungen* **25**: 70–84.
von Wilpert K, Mies E. 1995. The influence of stand structure and tree species on mineral cycling. In *Nutrient Uptake and Cycling on Forest Ecosystems; Ecosystem Research Report 21*, Nielsson O, Hüttl RF, Johansson UT, Mathy P (eds). Kluwer Academic Press: Dordrecht; 267–276.
von Wilpert K, Kohler M, Zirlewagen D. 1996. Die Differenzierung des Stoffhaushaltes von Waldökosystemen durch die waldbauliche Behandlung auf einem Gneisstandort des Mittleren Schwarzwaldes. *Mitteilungen der Forstlichen Versuchs- und Forschungsanstalt Baden-Württemberg* **197**: 134.
Waddington JM, Roulet NT, Hill AR. 1993. Runoff mechanisms in a forested groundwater discharge wetland. *Journal of Hydrology* **147**: 37–60.
Wilson GV, Jardine PM, Luxmoore RJ, Jones JR. 1990. Hydrology of a forested hillslope during storm events. *Geoderma* **46**: 119–138.
Zecharias YB, Brutsaert W. 1988. Recession characteristics of groundwater outflow and base flow from mountainous watersheds. *Water Resources Research* **24**: 1651–1658.

Copyright © 2001 John Wiley & Sons, Ltd.